Purification and Characterization of Ryanotoxin, a Peptide with Actions Similar to Those of Ryanodine

Jeffery Morrissette, Maryline Beurg, Manana Sukhareva, and Roberto Coronado
Department of Physiology, University of Wisconsin School of Medicine, Madison, Wisconsin 53706 USA

ABSTRACT We purified and characterized ryanotoxin, an ~11.4-kDa peptide from the venom of the scorpion *Buthotus judiacus* that induces changes in ryanodine receptors of rabbit skeletal muscle sarcoplasmic reticulum analogous to those induced by the alkaloid ryanodine. Ryanotoxin stimulated Ca^{2+} release from sarcoplasmic reticulum vesicles and induced a state of reduced unit conductance with a mean duration longer than that of unmodified ryanodine receptor channels. With Cs^+ as the current carrier, the slope conductance of the state induced by 1 μM ryanotoxin was 163 ± 12 pS, that of the state induced by 1 μM ryanodine was 173 ± 26 pS, and that of control channels was 2.3-fold larger (396 ± 25 pS). The distribution of substate events induced by 1 μM RyTx was biexponential and was fitted with time constants ~10 times shorter than those fitted to the distribution of substates induced by 1 μM ryanodine. Bath-applied 5 μM ryanotoxin had no effect on the excitability of mouse myotubes in culture. When 5 μM ryanotoxin was dialyzed into the cell through the patch pipette in the whole-cell configuration, there was a voltage-dependent increase in the amplitude of intracellular Ca^{2+} transients elicited by depolarizing potentials in the range of −30 to +50 mV. Ryanotoxin increased the binding affinity of [^{3}H]ryanodine in a reversible manner with a 50% effective dose (ED_{50}) of 0.16 μM without altering the maximum number (B_{max}) of [^{3}H]ryanodine-binding sites. This result suggested that binding sites for ryanotoxin and ryanodine were different. Ryanotoxin should prove useful in identifying domains coupling the ryanodine receptor to the voltage sensor, or domains affecting the gating and conductance of the ryanodine receptor channel.

INTRODUCTION

The ryanodine receptor forms a Ca^{2+} channel in the sarcoplasmic reticulum membrane of muscle cells and plays a key role in excitation-contraction coupling (Coronado et al., 1994; Meissner, 1994; Ogawa, 1994). In the latter process, a depolarization of the muscle cell surface membrane leads to the opening of ryanodine receptors and to the release of Ca^{2+} stored in the sarcoplasmic reticulum. This is followed by the mechanical shortening of the cell. The actual opening of the ryanodine receptor may occur by a voltage-dependent charge movement (Ebashi, 1991; Rios and Pizarro, 1991; McPherson and Campbell, 1993) or by Ca^{2+} entry into the cell (Stern and Lakatta, 1992; Wier et al., 1994), and both mechanisms are mediated by dihydropyridine receptors. A voltage-dependent mechanism is more prominent in adult skeletal muscle, whereas a mechanism dependent on Ca^{2+} entry is more prominent in adult cardiac muscle. On the other hand, a mixed form of ryanodine receptor activation by voltage and Ca^{2+} has been reported in embryonic muscle (Cognard et al., 1992). Studies of excitation-contraction coupling in dysgenic myotubes expressing chimeras of skeletal and cardiac cDNAs showed that the putative II-III cytoplasmic loop of the dihydropyridine receptor α_1 subunit was important for conferring a voltage or a Ca^{2+}-dependent Ca^{2+} release mechanism (Tanabe et al., 1990). Whether the cytoplasmic loop of the α_1 subunit interacts directly with the ryanodine receptor or its action is mediated by other junctional proteins is unknown.

The identification of functional domains on the ryanodine receptor is essential for understanding how voltage, Ca^{2+}, and perhaps other signals bring about the opening of the pore. However, the large size of the ryanodine receptor complex (~2000 kDa) has made this task slow and difficult. A Ca^{2+}-binding domain was identified between amino acid residues 4489 and 4499 of the skeletal ryanodine receptor. The functional significance of this domain was suggested by experiments in which a polyclonal antibody against the Ca^{2+}-binding sequence increased the ligand sensitivity of ryanodine receptor channels (Chen et al., 1993). A high-affinity binding site for the alkaloid ryanodine was located on a 76-kDa carboxy-terminal fragment most likely between Arg-4475 and the carboxy-terminal end (Witcher et al., 1994; Callaway et al., 1994). Based on the drastic modifications produced by the alkaloid, this domain may be critically involved in controlling the channel kinetics and the conductance of the pore. Numerous peptide-binding domains also seem to be present, as demonstrated by the tight and specific interactions of ryanodine receptors with FK506 binding protein (Jayaraman et al., 1992), small and large peptides from venoms (Morrissette et al., 1995; H. Valdivia et al., 1992), and α_1 II-III loop peptides (Lu et al., 1994; El-Hayek et al., 1995). Identification of peptide-binding domains controlling the gating of ryanodine receptors may prove critical in determining the structural basis of skeletal-type excitation-contraction coupling, because a mechanical interaction of the dihydropyridine receptor and the skeletal type ryanodine receptor has been proposed to mediate Ca^{2+} release in this tissue (Rios et al., 1991).

Received for publication 23 October 1995 and in final form 22 April 1996.
Address reprint requests to Dr. Roberto Coronado, Department of Physiology, University of Wisconsin, 1300 University Ave., Madison, WI 53706. Tel.: 608-263-7487; Fax: 608-265-5512; E-mail: blmlab@vms2.macc.wisc.edu.

0006-3495/96/08/707/15 $2.00

Scorpion neurotoxins are generally small basic peptides, typically consisting of 60 to 70 amino acid residues that affect excitable membranes by specifically binding to ion channels (Adams and Swanson, 1994). Previous studies on the venom of the scorpion *Buthotus judaicus* indicated the presence of two Na^+ channel toxins (Lester et al., 1982). In current clamp experiments with an insect nerve preparation, *B. judaicus* insect toxin I (BJ IT-I) induced slight depolarization accompanied by spontaneous or repetitive firing of action potentials of normal amplitude and shape. On the other hand, *B. judaicus* toxin II (BJ IT-II) induced a gradual depolarization accompanied by a decrease in the amplitude of the action potential. Under voltage clamp, IT-I caused an increase in the Na^+ current, whereas IT-II decreased the Na^+ current (Lester et al., 1982).

Here we report the purification of a peptide from the venom of the scorpion *B. judaicus* that stimulated ryanodine receptor channels in cell-free recordings obtained by fusion of sarcoplasmic reticulum to planar bilayers. In addition, the peptide stimulated intracellular Ca^{2+} transients induced by the depolarization of skeletal muscle myotubes in culture. This novel peptide was named ryanotoxin or RyTx, based on the observation that the peptide activated ryanodine receptors by inducing a long-lived subconductance state that was functionally similar to the subconductance state induced by ryanodine. Part of this work appeared in abstract form (Morrissette and Coronado, 1994).

MATERIALS AND METHODS

Preparation of sarcoplamic reticulum

Junctional sarcoplasmic reticulum sedimenting between 35% and 45% sucrose (w/v) was prepared from rabbit back and thigh muscle as described elsewhere (Sukhareva et al., 1994). Membranes were stored in liquid nitrogen in 0.3 M sucrose, 0.1 M KCl, 5 mM Na-piperazine-*N,N'*-bis-2-ethanesulfonic acid (Na-PIPES), pH 6.8.

Purification of ryanotoxin

Two separate batches of ~500 mg of lyophilized *B. judaicus* venom were purchased from Alamone Laboratories (Jerusalem, Israel) and were stored under vacuum at −20°C for up to a year without a significant loss of activity. A total of 10 preparations of purified RyTx were made from these two batches of venom. Each preparation of RyTx was started from a separate venom stock solution prepared from ~100 mg of lyophilized venom at a time. The venom powder was resuspended in 3 ml of water followed by sonication in a bath-type sonicator for 10 min. The floating mucus and foam were removed by aspiration, yielding ~1.5 ml of a transparent solution. The protein concentration of the venom stock was adjusted to ~4 mg/ml and was kept frozen at −20°C for several weeks without a significant loss of activity. RyTx was purified in a gradient high-performance liquid chromatography (HPLC) system (System Gold; Beckman Instruments, San Ramon, CA) in three chromatographic steps. Venom peptides were eluted with acetonitrile gradients (described by the dotted lines in Fig. 1) prepared in 0.1% trifluoroacetic acid. Absorption peaks corresponding to the peptide elution pattern were monitored at 254 nm. Fractionated absorption peaks were dried under vacuum centrifugation at room temperature and resuspended in a minimal volume of glass-distilled deionized water. The activity of HPLC fractions was determined by [^{3}H]ryanodine binding, taking care that approximately the same A_{254}

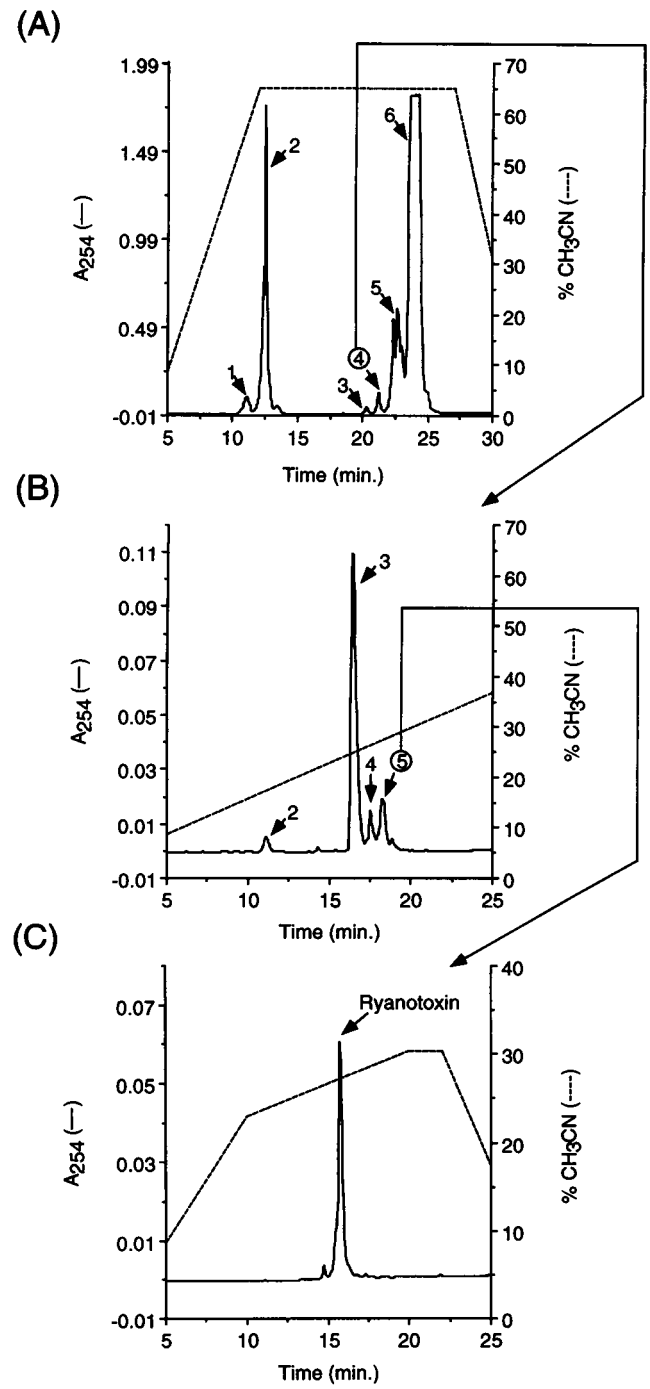

FIGURE 1 HPLC purification of ryanotoxin. (*A*) Chromatographic profile resulting from the injection of ~500 μg of water-soluble *Buthotus judaicus* venom into a preparative C_{18} reverse-phase column. Peptide fractions were eluted with an 8.75–65% acetonitrile gradient (dashed line) containing 0.1% trifluoroacetic acid run at a flow rate of 1.0 ml/min. (*B*) Chromatographic profile resulting from the injection of ~100 μg fraction 4 from *A* into an analytical C_{18} reverse-phase column. Fractions were eluted with an 8.75–45% acetonitrile gradient (dashed line) containing 0.1% trifluoroacetic acid run at a flow rate of 1.0 ml/min. (*C*) Chromatographic profile resulting from the reinjection of fraction 5 from *B* into the same analytical C_{18} reverse-phase column. Ryanotoxin was eluted with an 8.75–30% acetonitrile gradient containing 0.1% trifluoroacetic acid run at a flow rate of 1.0 ml/min.

units were assayed from each peak. Control binding in the absence of toxin was measured side by side in each assay.

The HPLC fractionation procedure during a single preparation of RyTx was as follows. Aliquots of ~200 μl of venom stock were injected into a preparative HPLC column (0.78 cm × 30 cm; mBondapac-Waters, Milford, MA). Peak 4 (Fig. 1 *A*) from six separate runs was pooled, dried, and resuspended in 300–500 μl of water. Aliquots of ~100 μl of resuspended peak 4 were injected into a analytical C_{18} HPLC column (0.46 × 25 cm; Vydac, Hesperia, CA). Peak 5 (Fig. 1 *B*) from three to five runs was pooled, dried, and resuspended in 200 μl of water. Aliquots of 50–100 μl of resuspended peak 5 were reinjected into a similar C_{18} HPLC column above and eluted with a shalower acetonitrile gradient described in Fig. 1 *C*. The ryanotoxin peak from two to four runs was pooled, dried, and resuspended in 200–300 μl of water at a concentration of 300–600 μg RyTx/ml. A stimulatory unit (1 S.U.) was defined as 1 pmol of specific [^{3}H]ryanodine binding stimulated by toxin after subtraction of the control [^{3}H]ryanodine binding without toxin. A typical venom stock measures 1500 S.U.; the activity was 250 S.U./mg stock venom. From this stock, a total of 900 S.U. was recovered in the purified RyTx fraction, and the activity was 15,000 S.U./mg RyTx.

[^{3}H]Ryanodine binding

Peptide fractions and controls without venom were assayed side by side in duplicate for 90 min at 37°C in 0.1 ml binding solution composed of 7 nM [^{3}H]ryanodine, 0.4 mg/ml SR, 0.2 M KCl, 1 mM Na_2EGTA, 0.995 mM $CaCl_2$, and 10 mM Na-PIPES, pH 7.2. The calculated free Ca^{2+} concentration of the binding buffer was 10 μM and was estimated as described elsewhere (Fabiato, 1988). Samples were filtered on Whatman GF/C glass fiber filters (Brandel, Gaithersburg, MD) and washed twice with 5 ml of distilled water using a Brandel cell harvester (Brandel, Gaithersburg, MD). Nonspecific binding was measured in the presence of 1 μM unlabeled ryanodine. In equilibrium binding experiments, incubations of SR and [^{3}H]ryanodine were extended to 17–19 h at room temperature in the same binding solution above plus 100 μg/ml bovine serum albumin (BSA), 100 μM phenylmethylsulfonyl fluoride, 200 μM benzamide, 1 μg/ml leupeptin, and 1 μg/ml pepstatin A. Nonspecific binding was determined in the presence of 100 μM unlabeled ryanodine.

Single-channel recordings

Planar lipid bilayers were formed by using a decane solution composed of 10 mg/ml brain phosphatidylethanolamine and 10 mg/ml brain phosphatidylserine (Avanti Polar Lipids, Alabaster, AL). The lipid solution was spread over a 300-μm-diameter aperture separating two aqueous chambers. SR was added to the *cis* solution composed of 240 mM $CsCH_3SO_3$, 10 mM CsCl, and 10 mM HEPES-Tris, pH 7.2. The *trans* solution was composed of 40 mM $CsCH_3SO_3$, 10 mM CsCl, and 10 mM HEPES-Tris, pH 7.2. The volume of the chamber to which the *cis* solution and toxin were added was ~300 μl, and that of the *trans* solution was 3 ml. Channel incorporation was assisted by breakage and reformation of the bilayer in the presence of SR and the $CsCH_3SO_3$ *cis*-to-*trans* gradient (Coronado et al., 1994). This procedure resulted in a partial dissipation of the original Cs^+ gradient established across the bilayer. Hence, the single-channel reversal potentials were less negative than the Cs^+ equilibrium potential of −38 mV. The *cis* and *trans* Cs^+ concentrations estimated by measuring the conductivity of samples of *cis* and *trans* solutions at the end of a typical experiment were in the following ranges: *cis*, 160–180 mM, and *trans*, 60–65 mM. The free Ca^{2+} of the *cis* solution was ~4 μM, as determined with a Ca^{2+}-sensitive electrode. The *cis* chamber was connected via an Ag/AgCl electrode to the headstage input of a List L/M EPC 7 amplifier (Medical Systems, Greenvale, NY). The *trans* solution was held at ground using the same electrode arrangement. Recordings were filtered at 1 kHz with a low-pass Bessel filter and stored on VCR tape. Recordings were digitized at 5 kHz for analysis. Single-channel events were identified using Transit 1.0 software (Baylor College of Medicine, Houston, TX), which uses a slope threshold to detect the opening and the closing event and a relative amplitude threshold to eliminate spurious transitions derived from baseline noise. Brief events identified by a single digitized sample of current flanked by two samples of baseline current were excluded from the amplitude histograms and lifetime distributions.

Primary cultures of mouse myotubes

Primary cultures of mammalian skeletal muscle cells were prepared from the hind limbs of 18-day mouse fetuses according to a procedure described elsewhere (Takekura et al., 1994), with some modifications. Mechanically dissociated muscles were incubated for 9 min at 37°C in Ca^{2+}/Mg^{2+}-free Hanks' balanced salt solution (136.9 mM NaCl, 3 mM KCl, 0.44 mM KH_2PO_4, 0.34 mM $NaHPO_4$, 4.2 mM $NaHCO_3$, 5.5 mM glucose, pH 7.2) containing 0.25% (w/v) trypsin and 0.05% pancreatin. After gentle aspiration and centrifugation, mononucleated cells were resuspended in plating medium containing 78% Dulbecco's modified Eagle's medium with low glucose (Gibco BRL, Gaithersburg, MD), 10% horse serum (Sigma, St. Louis, MO), 10% fetal bovine serum (Sigma), and 2% chicken embryo extract (Gibco BRL) and plated on glass coverslips at a density of 1 × 10^4 cells/dish. Culture were grown at 37°C, in 98% H_2O and 10% CO_2. After the fusion of myoblasts (6 days), the medium was replaced with contraction medium (88.75% Dulbecco's modified Eagle's medium, 10% horse serum, 1.25% chicken embryo extract), and cells were incubated in lower CO_2 (5%) atmosphere. All media contained 0.5% w/v penicillin and streptomycin.

Single-cell recordings and measurements of intracellular Ca^{2+}

Whole-cell recordings were made in a Axopatch 1D patch clamp with a 50-MΩ feedback resistor (Axon Instruments, Foster City, CA). The recording chamber was mounted on the stage of an inverted microscope for simultaneous measurement of cell fluorescence. Standard patch-clamp electrodes (2–5 mΩ) were used to establish the whole-cell configuration and to dialyze RyTx into the cell. External RyTx was added to the bath solution in Krebs superfusion medium. Action potentials and intracellular Ca^{2+} transients were recorded at room temperature under current-clamp in 8–10-day-old cultures of mouse skeletal myotubes superfused with a standard Krebs solution consisting of (in mM) 136 NaCl, 5 KCl, 2 $CaCl_2$, 1 $MgCl_2$, 10 HEPES (pH 7.4). The pipette solution was (in mM) 140 KCl, 5 $MgCl_2$, 10 HEPES/Tris. Cells were held at −80 mV and depolarized by 16-ms current pulses of 1 to 5 nA given at 2-s intervals. The data were filtered at 3 kHz and digitized at 50 μs per point. Acquisition was performed with a TL1 DMA interface controlled by pCLAMP 6.0 software (Axon Instruments). Ca^{2+} transients were additionally recorded under voltage clamp in cells superfused with a standard Ca^{2+} current recording solution consisting of (in mM) 130 tetraethylamonium methanesulfonate, 10 $CaCl_2$, 1 $MgCl_2$, and 10 HEPES (pH 7.4). The pipette solution consisted of (in mM) 140 Cs-aspartate, 5 $MgCl_2$, 0.1 EGTA, and 10 3-(*N*-morpholino)propanesulfonic acid (pH 7.2). Ca^{2+} transients in cells held under voltage clamp were elicited by a voltage pulse of variable amplitude and a fixed duration of 50 ms delivered every 40 s. The holding potential was −80 mV. Intracellular Ca^{2+} was measured by microfluorimetry of fura-2, using a dual alternating excitation wavelength illuminator attached to an inverted micropscope (Photon Technology International, London, ON, Canada). After a whole-cell recording configuration was established, a slit of 40 × 70 mm was adjusted toward the center of the cell and away from the patch pipette. Fluorescence emission passing through the slit area was guided to a photomultiplier tube. Fluorescence emission was separated from excitation by using a dicroic cube with a 400-nm dicroic mirror and a 510/20 emission barrier filter. Emission ratios in response to alternate 340/380 nm excitation were taken at a rate of 200 ratios/s. In current-clamp and voltage-clamp experiments, cells were loaded with 0.1 mM fura-2 AM (Molecular Probes, Eugene, OR) for 20 min at room temperature. The amplitudes of Ca^{2+} transients are expressed, as as suggested elsewhere

(Grouselle et al., 1991), as normalized fluorescence ratios. Each 340/380 fluorescence ratio aquired during the voltage or current pulse, Rt, was divided by the fluorescence ratio of the cell at rest before the stimulus, Rto. Controls performed in a quartz cuvette indicated that 5 μM RyTx did not change the fura-2 fluorescence emission at 340 or 380 nm excitation.

Sarcoplasmic reticulum Ca^{2+} release

Ca^{2+} release from SR vesicles was measured using the Ca^{2+} indicator dye fura-2 (Molecular Probes) in a 0.3-ml cuvette mounted on a spectrofluorimeter. Excitation wavelengths were 340 nm and 380 nm, and the emitted fluorescence spectra were recorded with a Hitachi F-2000 spectrofluorimeter (Hitachi, Danbury, CT). In each assay, an SR sample of 150 μg was actively loaded with Ca^{2+} in a solution composed of 100 mM KCl, 5 mM phosphocreatine, 5 μg/ml creatine phosphokinase, 0.5 μM fura-2 (free acid), 1 or 2 mM ATP, and 20 mM HEPES-Tris (pH 7.2) at 25°C. Ca^{2+} was present in the loading solution at contaminant levels in the range of 1–10 μM. The Ca^{2+} release transients were calibrated by a ratiometric method previously described (Grynkiewicz et al., 1985).

Gel electrophoresis

Sodium dodecyl sulfate (SDS)-polyacrylamide gel electrophoresis was performed as described elsewhere (Laemmli, 1970). Samples were incubated for 10 min at 80°C in 2% SDS, 2% b-mercaptoethanol, 10% glycerol, and 10 mM Tris (pH 6.8). Samples were run on a 6–20% linear polyacrylamide gradient. Gels were stained with 0.05% Coomassie blue in 10% acetic acid. Molecular weight standards were always run on two separate lanes of the same gel: myosin, M_r 200,000; b-galactosidase, M_r 116,250; phosphorylase b, M_r 97,400; BSA, M_r 66,200; ovalbumin, M_r 45,000; carbonic anhydrase, M_r 31,000; soybean trypsin inhibitor, M_r 21,500; lysozyme, M_r 14,000.

Chemicals and abbreviations

Deionized, glass-distilled water was used in all solutions. Na_2ATP and AMP-PCP (β,γ-methyleneadenosine 5′-triphosphate) were from Sigma. Ryanodine and CHAPS were from Calbiochem (San Diego, CA). Ruthenium red (Ruthenium III chloride oxide) was from Alpha Products (Andover, MA). Brain phosphatidylethanolamine and brain phosphatidylserine were from Avanti Polar Lipids. Penicillin, streptomycin, trypsin, pancreatin, phosphocreatine, and creatine phosphokinase were from Sigma. [^{3}H]Ryanodine (60 Ci/nmol) was from Du Pont-New England Nuclear (Wilmington, DE).

Protein assay

Protein concentration was determined by the Bradford method, with a Bio-Rad kit (Richmond, CA), with bovine serum albumin as the standard.

Curve fitting

Curve fitting was done using the standard Marquardt-Levenberg algorithm provided by Sigmaplot 2.0 (Jandel, San Rafael, CA) or DeltgaGraph 3.0 (DeltaPoint, Monterey, CA).

RESULTS

Purification of ryanotoxin

Ryanotoxin was purified by HPLC, using the stimulation of [^{3}H]ryanodine binding to junctional SR as the index of toxin activity. Fig. 1 *A* shows the chromatographic profile of ~500 μg of stock venom fractionated on a preparative C_{18} reverse-phase HPLC column. Fractions indicated by arrows were eluted using a 8.75–65% acetonitrile gradient (dashed line), dried under vacuum centrifugation, and resuspended in a minimal volume of water. The activity of each fraction was determined by a [^{3}H]ryanodine binding assay carried out for 90 min at 37°C. Because [^{3}H]ryanodine binds preferentially to the open state of the channel (Imagawa et al., 1987; Inui et al., 1988; Pessah et al., 1986), venom fractions that increased [^{3}H]ryanodine binding may have opened the channel, whereas those that decreased binding may have closed the channel. In this manner, we screened HPLC fractions that could potentially affect channel activity and determined that fraction 4 of Fig. 1 *A*, and to a lesser extent fraction 5, stimulated [^{3}H]ryanodine binding 1.2- to 2-fold, depending on the concentration. Other fractions in the profile inhibited [^{3}H]ryanodine binding (fractions 1 and 6) or had no effect (fractions 2 and 3). Fraction 4 (Fig. 1 *A*) was purified further using an analytical C_{18} reverse-phase column. Fig. 1 *B* shows the chromatographic profile resulting from the injection of ~100 μg of fraction 4 (Fig. 1 *A*) into the analytical column. Nearly all of the stimulatory activity was recovered in a single A_{254} absorbance peak corresponding to fraction 5 of Fig. 1 *B*. After reinjection of peak 5 into an analytical C_{18} reverse-phase column, this fraction eluted as a single homogeneous peak with a retention time of ~16 min in a 8.75–30% acetonitrile gradient (Fig. 1 *C*). The stimulatory [^{3}H]ryanodine binding activity purified according to the three steps of HPLC chromatography described above was identified as ryanotoxin or RyTx. The elution profiles shown in Fig. 1 were consistently observed in 10 separate purifications of RyTx (see Materials and Methods).

To determine the polypeptide composition, a sample of 5 μg of purified RyTx was run on a linear 6–20% SDS-polyacrylamide gel under disulfide-reducing conditions. Fig. 2 *A* shows that RyTx (*lane 1*) migrated as an apparently single polypeptide of M_r ~11.4 kDa, determined from a semilog plot (Fig. 2 *B*) of the mobility of RyTx and the indicated markers run on the same gel. On the other hand, the water-soluble unfractionated venom (Fig. 2 *A*, *lane 2*) consisted of high- and low-molecular-weight peptides in the range of ~130 kDa to 6 kDa, with the majority of the peptides concentrated at ~10 KDa. In separate gel runs (not shown), samples of 20 μg RyTx migrated as a single band with a mobility similar to that above, although the staining pattern was more diffuse. RyTx was thus largely free of high-molecular-weight peptides present in the venom and was likely to consist either of a single polypeptide or several distinct polypeptides of highly similar molecular weights and HPLC elution profiles. Based on the total A_{254} absorbance units of the venom stock and the amount of protein recovery in the purified sample, RyTx represented, respectively, ~0.5% and ~2% of the total water-soluble venom. The enrichment in [^{3}H]ryanodine binding stimulatory activity in the purified RyTx fraction was approximately 30-fold, and the recovery of the stimulatory activity in the RyTx fraction was typically 60% (see Materials and Methods).

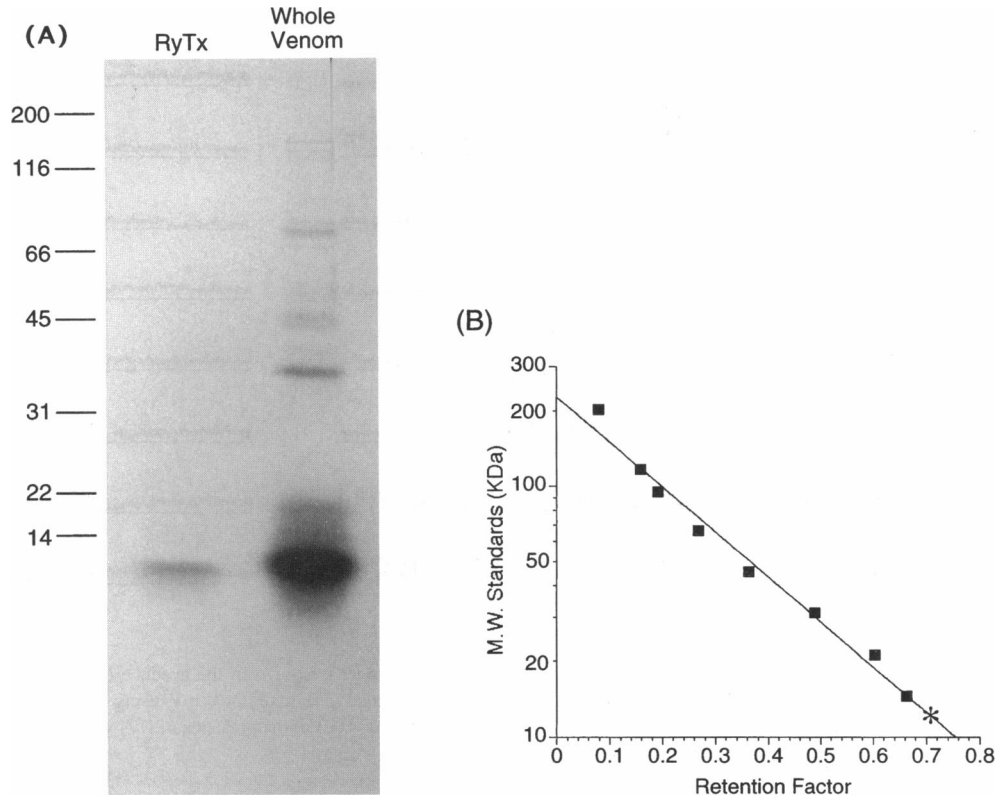

FIGURE 2 (*A*) Electrophoretic analysis of ryanotoxin. Coomasie blue staining of a 6–20% SDS polyacrylamide gel. Lane 1: 2.5 μg RyTx. Lane 2: 5 μg *Buthotus judaicus* venom stock solution. Molecular weight markers in the same gel are indicated by lines. (*B*) Molecular weight markers are plotted as a semilog function of the retention in the gel, the latter defined as the distance moved by the marker from the loading trough divided by the distance between the loading trough and the dye front. The asterix indicates the mobility of RyTx resulting in a calibrated apparent molecular mass of 11.4 kDa.

However, the calculated enrichment of activity and yield is only approximate, because the stock venom was composed of peptides that stimulated and inhibited [^{3}H]ryanodine binding, and part of the stimulatory activity of purified RyTx probably was masked in the unfractionated venom.

Characteristics of the ryanotoxin-modified ryanodine receptor channel

The left and center panels of Fig. 3 show recordings of a ryanodine receptor during a control period, and after the addition of 1 μM ryanotoxin to the *cis* solution. The main effect of the peptide was to induce a conductance state with a unitary value ~40% lower than that seen during the control period. Furthermore, the mean duration of the substate was much longer than that of the open state seen during controls. Thus, in the presence of the peptide, the channel alternated between closed, open, and substate configurations, with the largest fraction of time spent in the substate. The substate always appeared within seconds of peptide addition, and in most cases, during the period of solution stirring, which lasted no more than 15 s. Because ryanodine is known to induce a long-lived substate, we compared the characteristics of both substates under the same recording conditions. The right panel of Fig. 3 shows recordings from a separate ryanodine receptor modified by 1 μM ryanodine. In agreement with reports describing the effect of similar concentrations of the alkaloid on skeletal ryanodine receptors (Imagawa et al., 1987; Lai et al., 1989), ryanodine induced a substate with an extremely large probability of occurrence, which in this case was >0.95.

Fig. 4 shows amplitude histograms of all nonclosed events at 0 mV ($n > 1000$ in each histogram) for a control recording and for recordings of RyTx- and ryanodine-modifed channels. Control events were clustered into a single peak with a mean of ~11 pA, which represented the unitary current of the open state. A trailing edge below the mean represented both brief events attenuated by the filter cutoff frequency of 1 kHz (−3 dB) and events of low amplitude that are clearly present in Fig. 3 and elsewhere (Morrissette et al., 1995). Events collected from a RyTx-modified channel were distributed into a peak of ~10.4 pA corresponding to the toxin-unmodified open state and a peak of ~3.5 pA representing the mean unitary current distribution of the substate induced by RyTx. On the other hand, events collected from a ryanodine-modified channel had a somewhat broader distribution, with a mean of ~3.9 pA representing the mean unitary current of the substate induced by ryanodine. Events representing the ryanodine-unmodified open channel were not present. The similarity in unitary current

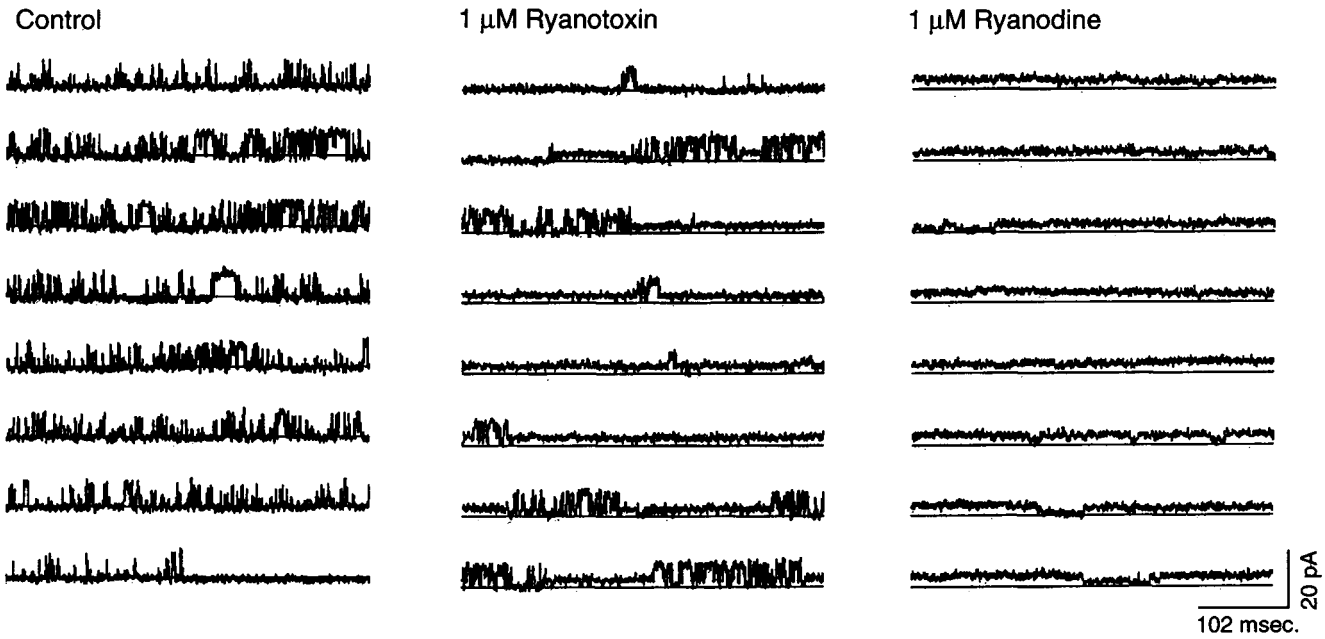

FIGURE 3 Effect of ryanotoxin on skeletal ryanodine receptor channels. The same channel is shown in the absence (control) and presence of 1 μM ryanotoxin. A separate channel is shown in the presence of 1 μM ryanodine. All recordings were made at 0 mV using Cs^+ as the current carrier. The baseline is indicated by the solid line. The probability of the open state was 0.21 in control and 0.13 in the presence of RyTx. The probability of the substate was 0.38 in the presence of RyTx and 0.90 in the presence of ryanodine.

amplitude of the substates induced by RyTx and ryanodine was confirmed at several voltages above and below the reversal potential (Fig. 5). Current-voltage curves in Fig. 5 *A* are for the open state during the preceding control period (*squares*), and for the substate induced in the same channel by RyTx (*circles*). A linear fit of the data showed that RyTx induced a substate with a mean conductance of 163 pS. This value represented a 2.37-fold reduction in conductance (387/163) relative to the conductance of open state during the preceding control period. On the other hand, the reversal potential of the substate was the same as that of the control open state and suggested that RyTx did not noticeably change the ionic selectivity of the channel. Current-voltage curves for a ryanodine-modified channel, and for the open state before alkaloid addition, are shown in Fig. 5 *B*. The substate induced by ryanodine had a mean conductance of 174 pS, which represented a 2.32-fold reduction in conductance (405/174) relative to its control. As in the case of RyTx, the reversal potential of the ryanodine-modified channel remained invariant. A Student's *t*-test analysis of two populations with different sample means showed that neither the conductance of the substates induced by RyTx or ryanodine (163 ± 12 pS versus 173 ± 26 pS), nor the conductance of the open state during the two control periods (387 ± 35 pS versus 405 ± 14 pS) was significantly different ($p < 0.05$). From these results we concluded that ryanotoxin and ryanodine induced conductance states of identical unitary value.

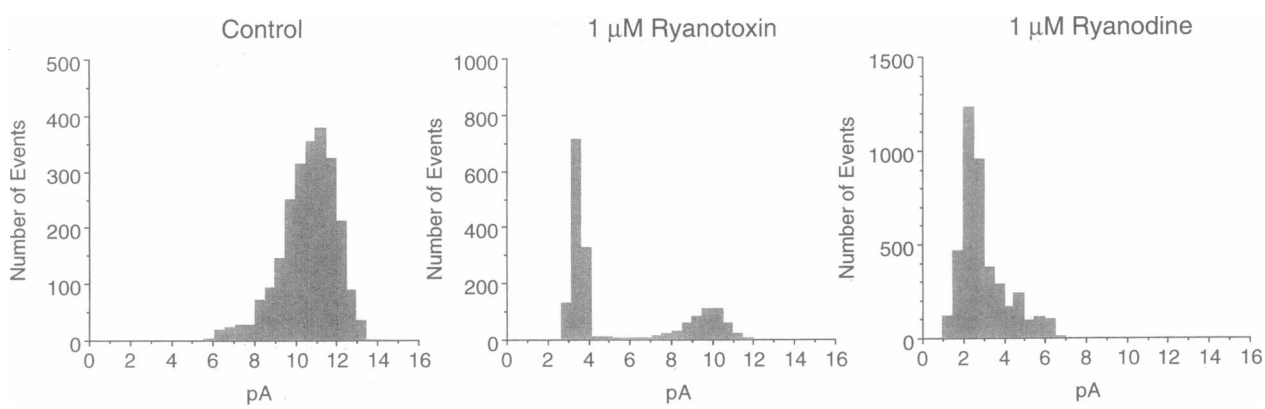

FIGURE 4 Amplitude distributions of ryanotoxin- and ryanodine-modified openings. The amplitude of unitary events at 0 mV was binned every 0.5 pA. Control (n = 2353 events), 1 μM RyTx (n = 1558 events), 1 μM ryanodine (n = 4107 events).

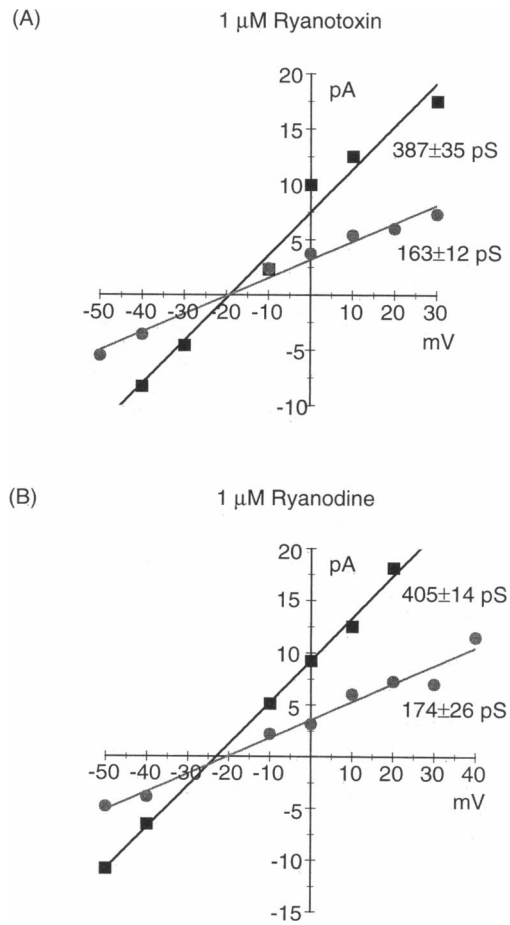

FIGURE 5 Current-voltage relationships of ryanotoxin- and ryanodine-modified openings. Current-voltage curves are shown for the control channel (squares) and for the substate (circles) induced in the same control channel by 1 μM RyTx (*A*) or by 1 μM ryanodine (*B*). The mean and standard error of a linear fit are shown for each curve.

Even though substate conductances were identical, the RyTx-modified channel differed from the ryanodine-modified channel in other respects. For example, the recordings of Fig. 3 clearly showed that the RyTx-modified channel could undergo transitions between the substate and a large apparently unmodified open state or between closed and open states, whereas the ryanodine-modified channel could not. Thus, we investigated the kinetics of the RyTx- and ryanodine-modified channels. Open events during control (Fig. 6 *A*), and large openings after exposure to ryanotoxin (Fig. 6 *B*) had distributions that were clearly monoexponential, with nearly the same mean open time. This result confirmed that some unmodified open events were indeed present after exposure to RyTx. Distributions of substate events induced by ryanotoxin (Fig. 6 *C*) as well as by ryanodine (Fig. 6 *D*) were biexponential. Because the mean duration of the substate induced by ryanotoxin was 5- to 10-fold shorter than that induced by ryanodine, the kinetic modification induced by ryanodine appeared to be much more stable than that induced by the peptide.

The presence of an open state in the ryanotoxin-modified channel with the same conductance and mean duration as that of control channels suggested that ryanotoxin could freely associate and dissociate from the channel. Thus when ryanotoxin was bound to the channel, the substate would be formed, but when it dissociates from its binding site, the channel may transiently open and close with unmodified kinetics. Inspection of the recordings further indicated that ryanotoxin was likely to dissociate either from the closed state or from the open state, because transitions between the substate and the open state and between the substate and the close state were almost equally represented in the data (not shown). We sought to test the hypothesis that ryanotoxin could dissociate from the channel by determining the sensitivity of ryanotoxin-modified channels to inhibition by ruthenium red. It has been shown that ruthenium red can irreversibly block open-closed transitions of control channels, but that the substate induced by ryanodine is insensitive to ruthenium red (Imagawa et al., 1987; Nagasaki and Fleischer, 1988; Ma, 1993). In agreement with the previous results, Fig. 7 *A* shows that control openings were rapidly inhibited by 1 μM ruthenium red added to the *cis* solution. On the other hand, the probability of occurrence of the substate induced by ryanodine shown in Fig. 7 *B* was unchanged by ruthenium red. Fig. 7, *C* and *D*, shows an experiment in which 1 mM ruthenium red was added to a ryanotoxin-modified channel and activity was followed thereafter. Open events (Fig. 7 *C*) and substate events (Fig. 7 *D*) were inhibited by ruthenium red with a significant delay, which in this case was ~40 s after the completion of solution mixing. The fact that channel inhibition was observed indicated that a ruthenium red-sensitive open state and/or substate was indeed present in the RyTx-modified channel. Furthermore, the fact that inhibition occurred with a delay not seen in controls suggested that the open state, which had a low probability of occurrence, and not the substate, which had a high probability of occurrence, was the target of ruthenium red. These results provided an electrophysiological indication that RyTx may in fact transiently dissociate from the channel, thus making the open RyTx-free channel available to inhibition by ruthenium red.

Stimulation of SR Ca^{2+} release by ryanotoxin

If RyTx generated a long-lived conducting state in the ryanodine receptor, incubation of SR with the peptide should result in a release of stored Ca^{2+}. To determine whether this was the case, we used the fluorescent Ca^{2+} indicator fura-2 to monitor Ca^{2+} release from the SR spectrofluorimetrically. Ca^{2+} was actively loaded into the SR by the addition of 2 mM MgATP to a cuvette containing 0.5 mM fura-2 (free acid), 0.4 mg/ml SR, contaminant-free Ca^{2+} (1 to 3 μM), 150 mM KCl, 5 mM phosphocreatine, 5 mg/ml creatine phosphokinase as an ATP-regenerating system, and 20 mM HEPES-Tris (pH 7.2). Experiments were terminated with additions of 1 mM Ca^{2+} and 10 mM EGTA

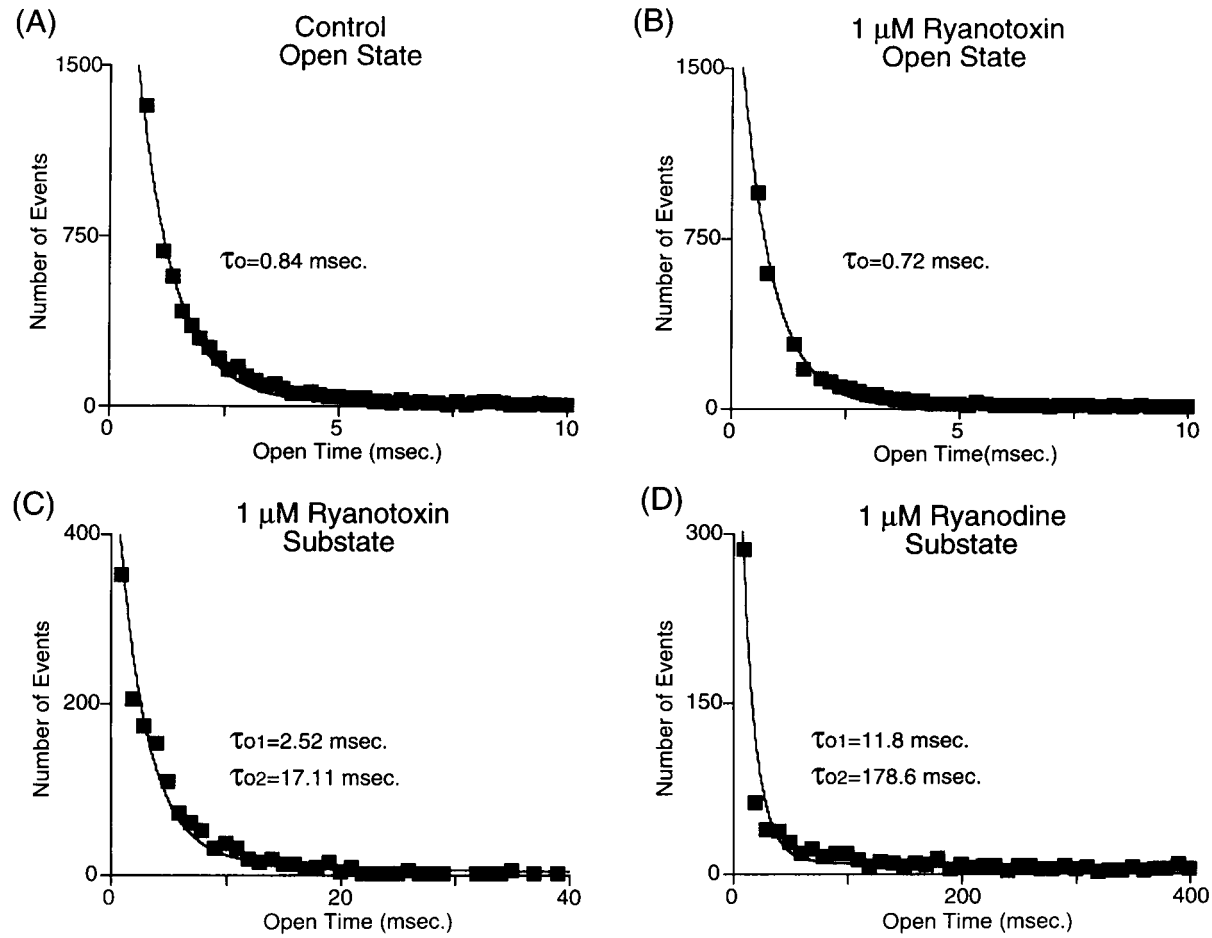

FIGURE 6 Time distributions of ryanotoxin- and ryanodine-modified open events. Distributions of 5702 open events during a control period (*A*) and 1420 open events after the addition of 1 μM RyTx (*B*) are from the same channel. Distributions of 1420 substate events induced by 1 μM RyTx (*C*) or 733 events induced by 1 μM ryanodine (*D*) are from separate channels.

to calibrate the extravesicular free Ca^{2+} according to the ratiometric technique (Grynkiewicz et al., 1985). As shown in each of the four traces of Fig. 8, the addition of ATP resulted in a large decrease in extravesicular free Ca^{2+}, which was almost exclusively due to the stimulation of the SR Ca^{2+} pump. The addition of ATP in the absence of SR resulted in a small decrease in fluorescence due to ATP-Ca^{2+} binding, which was on the order of ~0.02 nmol of free Ca^{2+}. This value was small compared to the active sequestration, which was typically in the range of 0.35 to 0.75 nmol of free Ca^{2+}. Uptake had a rate of 4 to 10 nmol Ca^{2+}/mg SR/min, which agreed well with previous results (C. Valdivia et al., 1992). Controls using 10 μM thapsigargin demonstrated that >50% of Ca^{2+} accumulated in the SR could be released within 30 s of the addition of drug. As shown in Fig. 8 *A*, the addition of 10 mM caffeine after completion of the Ca^{2+} loading phase resulted in a sudden release of stored Ca^{2+} equivalent to ~0.8 nmol Ca^{2+}/mg SR. The release was followed by a slower Ca^{2+} removal phase lasting several minutes as the released Ca^{2+} was driven back into vesicles by the Ca^{2+} pump. As expected from a ryanodine receptor-mediated process, the caffeine-induced release could be blocked by the prior addition of 1 μM ruthenium red (Fig. 8 *B*). In a separate experiment, the addition of 100 nM RyTx to the cuvette after completion of the Ca^{2+} loading phase resulted in the release of ~0.53 nmol Ca^{2+}/mg SR (Fig. 8 *C*). The Ca^{2+} release induced by the peptide was blocked by ruthenium red (Fig. 8 *D*), which demonstrated that the release occurred by the activation of ryanodine receptors. These results demonstrated that RyTx, like caffeine, could promote a significant release of SR stored Ca^{2+}, presumably by opening many ryanodine receptors simultaneously, so that the Ca^{2+} removal rate set by the Ca^{2+} pump was overcome by the Ca^{2+} release rate enhanced by the toxin.

Stimulation of Ca^{2+} transients by ryanotoxin in skeletal muscle myotubes

To determine the effectiveness and specificity of RyTx in cells, we performed recordings in primary cultures of mouse myotubes. Fig. 9 *A* shows action potentials in a control myotube bathed in Krebs solution and separately in a myo-

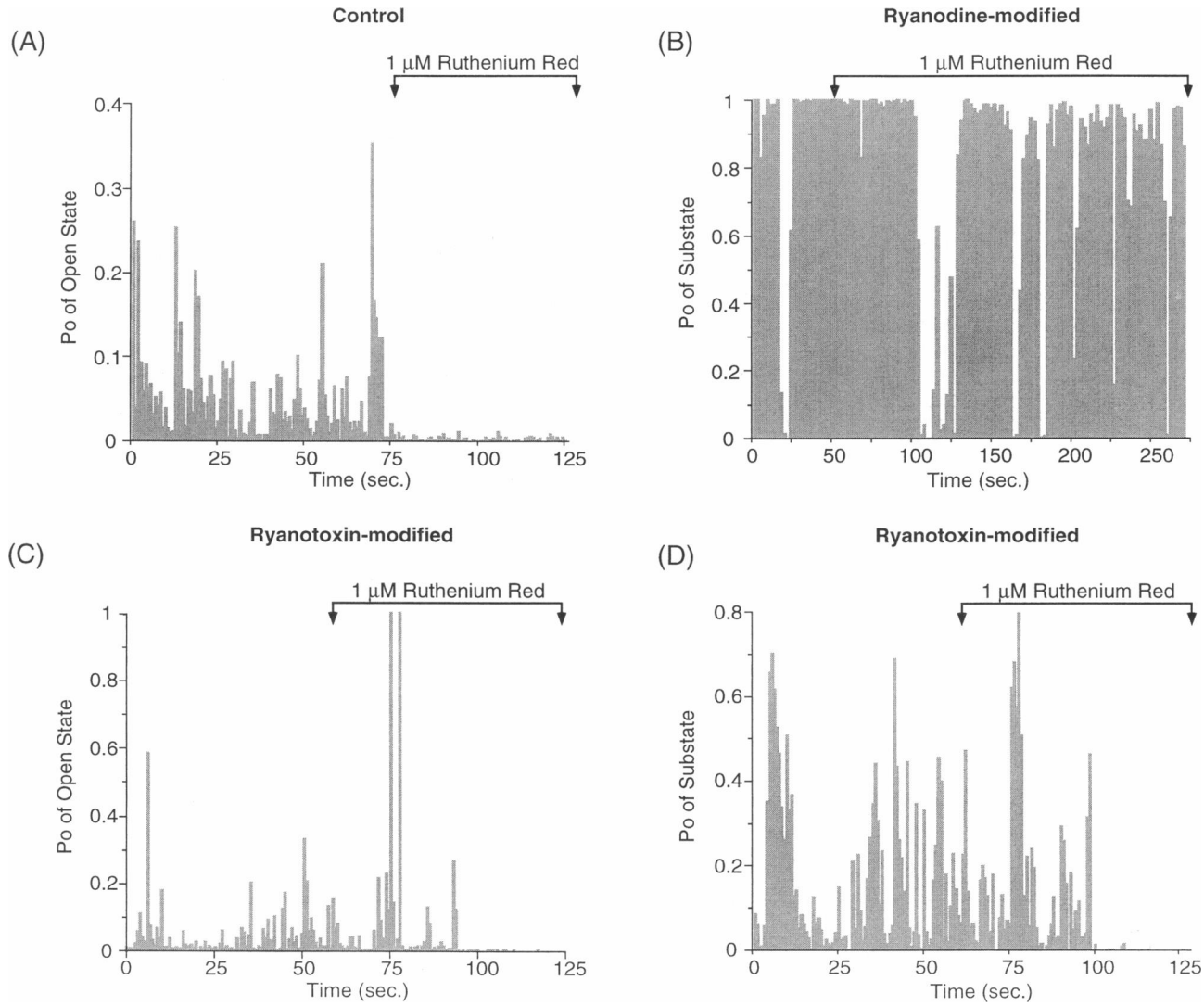

FIGURE 7 Diary of event probability modified by ruthenium red. Open or substate probability was measured continuously during intervals of 683 ms and was plotted as a bar of length 0 to 1. Recording period in the presence of *cis* 1 μM ruthenium red is indicated by arrows. Separate recordings are shown for a control (*A*), ryanodine-modified (*B*), and ryanotoxin-modified (*C*, *D*) channels.

tube exposed to Krebs solution containing 5 μM RyTx. Cells were maintained under current clamp at a holding current adequate to keep the resting potential at −80 mV. Action potentials (labeled 1 to 5) were each elicited by a current pulse of amplitude 1 to 5 nA with a constant increment of 1 nA from one pulse to the next. Thus, the action potential labeled 1 was elicited by 1 nA, whereas the action potential labeled 5 was elicited by 5 nA. Each pulse lasted 16 ms; these were given at intervals of 2 s. The initiation and termination of the current pulse are clearly visible in records 2 to 5 as a fast charge and discharge of the cell capacitance mounted on the time course of the action potential. As the amplitude of the stimulus increased, the delay in triggering the action potentials became equally short in the control and toxin-exposed myotubes. Furthermore, the shape of the action potential and maximum depolarization were not affected by the toxin. In addition, a comparison of the upstroke velocity in control and toxin-exposed cells indicated that this parameter remained unchanged (155 ± 45 V/s (n = 5 control cells) and 155 ± 39 V/s (n = 5 RyTx-exposed cells)). These results indicated that RyTx, at concentrations used in planar bilayer experiments, did not affect the fast Na^+ and K^+ current components of the skeletal muscle cell action potential and did not affect the Na^+ and K^+ gradients underlying the action potential. Fig. 9 *B* shows that when the peptide was dialyzed into cells through the patch pipette filled with 5 μM RyTx, there was a large potentiation of the Ca^{2+} transient elicited by a pulse to +30 mV. In these recordings, the cell was ruptured, and whole-cell voltage-clamp configuration was established 1–2 min before the recording of the Ca^{2+} transient. The time between rupturing of the cell with the pipette and the recording of the train of Ca^{2+} transients appeared sufficient for the peptide to diffuse out of the pipette and to increase

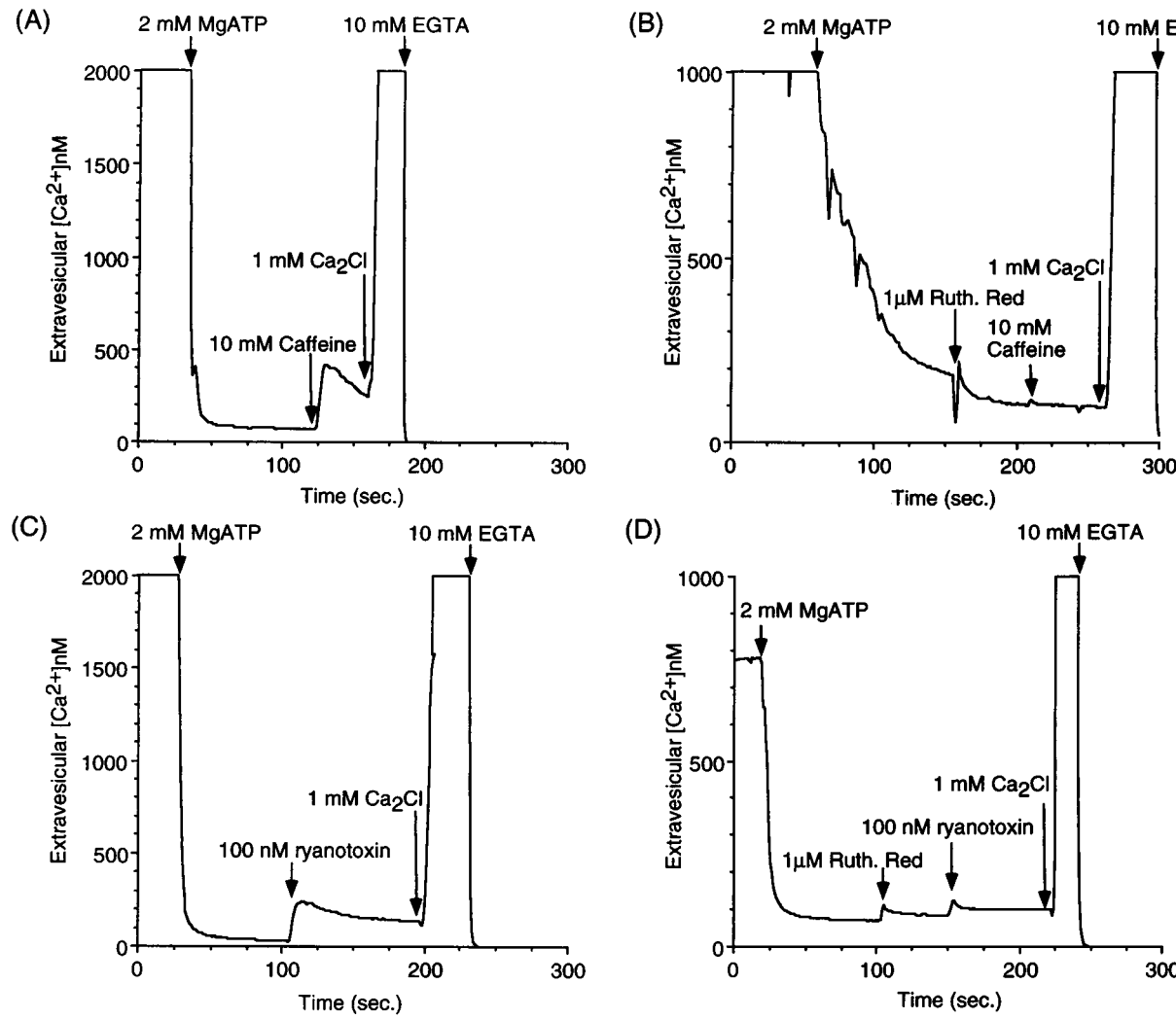

FIGURE 8 Stimulation of SR Ca^{2+} release by ryanotoxin. Ca^{2+} was actively loaded into the SR by 2 mM MgATP in the presence of 0.5 mM fura-2 (free acid), ~0.4 mg/ml SR, contaminant-free Ca^{2+} (1–3 μM), 150 mM KCl, 5 mM phosphocreatine, 5 mg/ml creatine phosphokinase, 20 mM HEPES-Tris, pH 7.2. (*A*) Ca^{2+} release induced by 10 mM caffeine. (*B*) Block of caffeine-induced Ca^{2+} release by 1 μM ruthenium red. (*C*) Ca^{2+} release induced by 100 nM RyTx. (*D*) Block of peptide-induced Ca^{2+} release by 1 μM ruthenium red. $CaCl_2$ (1 mM) and Na_2EGTA (10 mM) were added at the end of each experiment to determine F_{max} and F_{min}.

peak Ca^{2+}. Intracellular Ca^{2+} transients were elicited by voltage pulses of variable amplitude from −40 to +60 mV and a fixed duration of 50 ms. Between pulses there was a resting period of 40 s. In control cells, the Ca^{2+} transient monitored by fura-2 resulted in a doubling of the fluorescence 340/380 ratio relative to the resting ratio, and this increase was almost simultaneous with the onset of the pulse. However, the resting fluorescence ratio between pulses was unaffected by the toxin. The peak fluorescence was followed by a decay due to Ca^{2+} removal, which in control cells had a $t_{1/2}$ of 0.3 to 0.5 s and which agreed with previous reports (Grouselle et al., 1991; Garcia and Beam, 1994). RyTx produced a substantial delay in the onset of Ca^{2+} removal, increasing the $t_{1/2}$ 5- to 10-fold. The increase in peak Ca^{2+} during the transient was insignificant at −10 mV, but increased by ~4 fold and more at large positive potentials (Fig. 9 *C*). Only dialyzed but not externally applied toxin was capable of stimulating Ca^{2+} transients, suggesting that the peptide did not readily penetrate the cell membrane. These recordings demonstrated that RyTx selectively stimulated voltage-induce Ca^{2+} release without affecting the overall resting free Ca^{2+} nor the surface membrane currents controlling cell excitability.

Stimulation of [^{3}H]ryanodine binding by ryanotoxin

To investigate the ligand-binding properties of RyTx and the potential interaction between RyTx and ryanodine-binding sites, we took advantage of the fact that the rate of binding of [^{3}H]ryanodine is proportional to the number of open channels (Imagawa et al., 1987; Inui et al., 1988; Pessah et al., 1986). Accordingly, we measured the amount

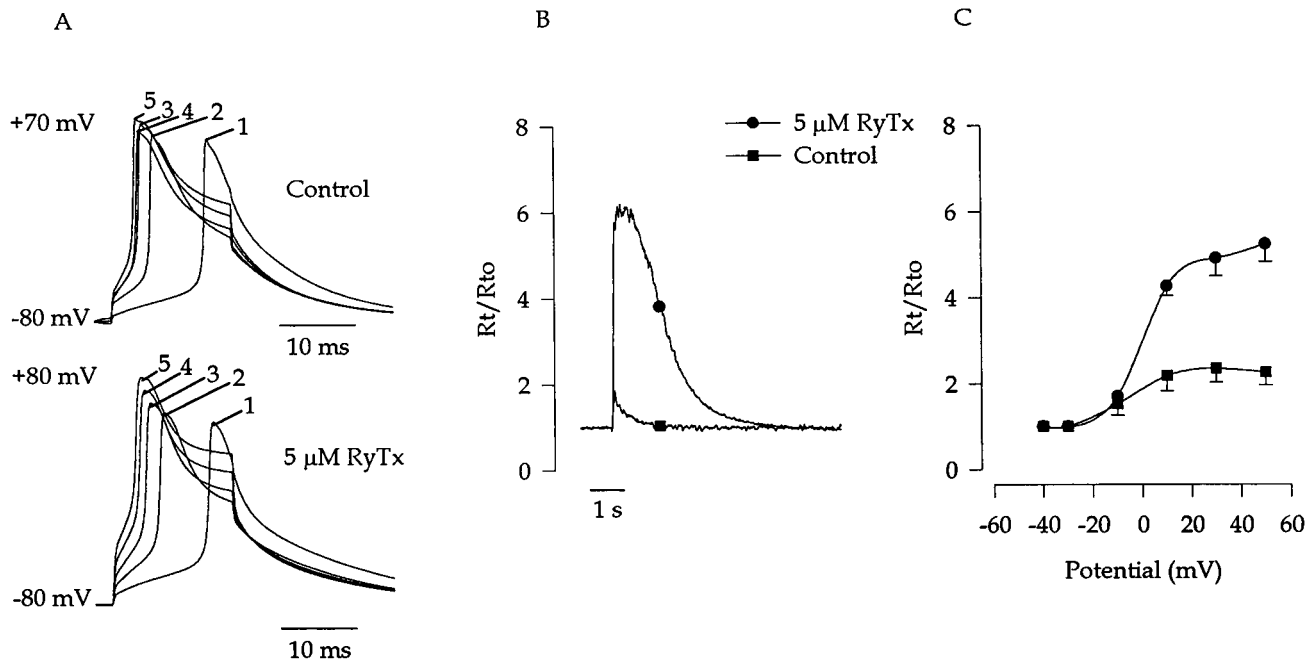

FIGURE 9 Stimulation of intracellular Ca^{2+} transients by ryanotoxin. (*A*) Action potentials in myotubes held under whole current-clamp in Krebs solution (control) or Krebs solution plus 5 μM RyTx. After whole-cell configuration was established, the holding current was adjusted such that the resting potential was −80 mV in all cases. Action potentials 1 through 5 were elicited by square current pulses of 16 ms of amplitude 1 through 5 nA, respectively. (*B*) Ca^{2+} transients in separate cells held under whole-cell voltage-clamp. The transient was elicited by a 50-ms voltage pulse to +30 mV. In the test cell (filled circles) RyTx was present in the pipette solution at the indicated concentration. (*C*) Average peak Ca^{2+} during Ca^{2+} transient elicited by the indicated step depolarization. Mean and SD of four control cells (squares) and three RyTx-loaded cells (circles). Rto corresponds to the fluorescence ratio at rest before each pulse and Rt to the peak ratio fluorescence.

of specifically bound [^{3}H]ryanodine at a fixed time before equilibrium and correlated changes in the binding activity of [^{3}H]ryanodine with changes in the number of channels opened by the peptide. As shown in Fig. 10, control binding was 1 to 2 pmol of [^{3}H]ryanodine bound/mg SR during a preestablished 90-min assay at 37°C. This binding represented a small fraction of the B_{max} at equilibrium, which was ~15 pmol/mg. RyTx at concentrations between 30 nM and 3 μM increased [^{3}H]ryanodine binding in a concentration-dependent manner from ~1.3 pmol/mg to ~3.8 pmol/mg or ~3-fold. The concentration that produced half-maximum stimulation was 200 ± 25 nM RyTx. The 3-fold increase in [^{3}H]ryanodine binding at saturating concentrations of RyTx correlated well with the increase in channel activity produced by RyTx in the micromolar range (see Discussion). These data demonstrated that the substate induced by RyTx represented a conformation favorable for the binding of the alkaloid. Fig. 11 shows that the stimulation of [^{3}H]ryanodine binding by RyTx was reversible, because removal of RyTx by extensive wash of the SR sample before incubation with [^{3}H]ryanodine restored the binding activity to control levels. This observation demonstrated that RyTx could readily dissociate from the channel and agreed with the inhibition of the RyTx-modified channel by ruthenium red described above.

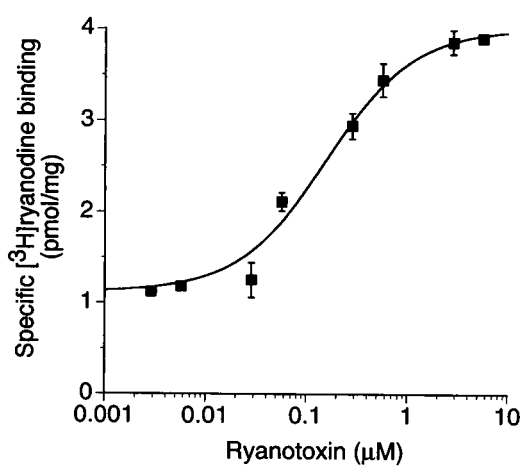

FIGURE 10 Stimulation of [^{3}H]ryanodine binding by ryanotoxin. Specific binding was determined in the presence of the indicated concentrations of RyTx. The solid line corresponds to a fit of the data according to a single-site isotherm containing an additional linear term for the control binding. Specific Binding = $B_{max}/(1 + K_d/[RyTx]) + B_{min}$, where B_{max} = 2.9 pmol/mg, B_{min} = 1.2 pmol/mg, and K_d = 0.16 μM.

In Fig. 12 we investigated the effect of RyTx on the binding of [^{3}H]ryanodine under equilibrium conditions to determine whether the peptide modified the alkaloid-binding affinity, the binding site density, or both. Because the rate at which [^{3}H]ryanodine binds to the receptor is extremely slow, overnight incubations of 17–19 h were required to reach equilibrium. Under these conditions, prote-

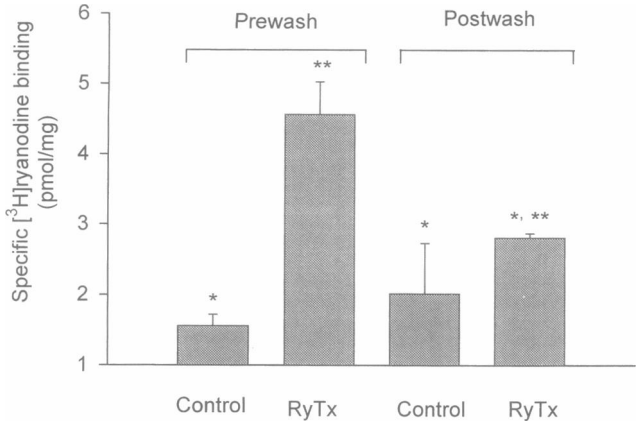

FIGURE 11 Reversible stimulation of [^{3}H]ryanodine binding by ryanotoxin. In prewash, three separate SR samples were incubated for 15 min in binding buffer without (control) or with 0.1 μM RyTx. All samples were incubated with 7 nM [^{3}H]ryanodine, and specific binding was determined at 90 min in duplicates of each sample. In postwash, three separate SR samples were incubated for 15 min in binding buffer without (control) or with 0.1 μM RyTx. Samples were pelleted and resuspended in binding buffer without peptide and incubated with 7 nM [^{3}H]ryanodine. By Student's *t*-test for the difference between two population means, each mean from an independent sample, any two bars with a single asterisk (*) were significantly different ($p < 0.01$), and any two bars with two asterisks (**) were not significantly different.

olysis of the receptor can lead to a decrease in binding activity (Wang et al., 1993). To minimize this problem, protease inhibitors and 100 μg/ml BSA were added to the incubation solution. Fig. 11 *A* shows the equilibrium binding of [^{3}H]ryanodine in the presence of 0.3 μM or 0.6 μM RyTx, and in the presence of the known activator AMP-PCP. The effect of the peptide was to produced a shift in the [^{3}H]ryanodine binding isotherm toward lower ryanodine concentrations. Furthermore, the shift produced by 1 mM AMP-PCP, which is known to bind to a site different from the ryanodine-binding site (Zorzato et al., 1990; Witcher et al., 1994; Callaway et al., 1994), was equal to that produced by 0.3 μM RyTx. The Scatchard analysis shown in Fig. 12 *B* indicates that the stimulation by RyTx or AMP-PCP was due exclusively to an increase in the affinity of [^{3}H]ryanodine for the binding site without a significant change in the B_{max}. In three separate experiments, the values of B_{max} (in pmol/mg) were 17 $\pm$ 2.2 (control), 15.1 $\pm$ 1.4 (AMPCP), 15.1 $\pm$ 1.5 (0.3 μM RyTx), and 16.2 $\pm$ 4.8 (0.6 μM RyTx). On the other hand, the apparent dissociation constant for [^{3}H]ryanodine decreased from 37.7 $\pm$ 4.9 nM in the control solution to 12.5 $\pm$ 1.2 nM in the presence of AMPPCP, 12.9 $\pm$ 1.3 nM in the presence of 0.3 μM RyTx, and 9.8 $\pm$ 3 nM in the presence of 0.6 μM RyTx. These data demonstrate that [^{3}H]ryanodine binds with increased affinity to the RyTx-bound receptor. Furthermore, the fact that RyTx did not displace but rather enhanced [^{3}H]ryanodine binding ruled out the possibility that the two ligands might share the same binding site on the receptor.

DISCUSSION

We purified and characterized ryanotoxin, an ~11.4-kDa peptide from the venom of the scorpion *Buthotus judaicus* that modifies the single-channel conductance and kinetics of skeletal ryanodine receptors and potentiates intracellular Ca^{2+} transients in myotubes. The fact that RyTx increased the binding affinity of [^{3}H]ryanodine and that ^{125}I-labeled RyTx (not shown) bound the solubilized ryanodine receptor complex suggested that binding sites for the peptide may be actually present on the surface of the receptor or in closely associated protein. RyTx migrated with a molecular weight larger than that of two neurotoxins purified from the same venom, namely BJ IT-I and BJ IT-II, with molecular masses of ~7 kDa (Lester et al., 1982). In addition, RyTx did not affect the upstroke velocity of the action potential in myotubes, indicating that RyTx was unrelated to the previously identified Na^+ channel toxins. Peptides that stimulated [^{3}H]ryanodine binding have been described previously in the venoms of the scorpions *Pandinus imperator* (H. Valdivia et al., 1992) and *Buthotus hottentota* (Morrissette et al., 1995). Imperatoxin A purified from *P. imperator* (H. Valdivia et al., 1992) and ButhA-1 and ButhA-2 purified from *B. hottentota* (Morrissette et al., 1995) differed from RyTx in their apparent molecular weights and in the fact that these peptides increased the open probability of skeletal ryanodine receptors without modifying the single-channel conductance. Furthermore, *B. judaicus* and *B. hottentota* venoms had the same peptide profile as shown in Fig. 1 *A*; however, ButhA-1 and ButhA-2 migrated with a peak equivalent to peak 5 of Fig. 1 *A* (Morrissette et al., 1995), whereas RyTx was purified from peak 4 of Fig. 1 *A*. These observations indicated that none of the stimulatory peptides previously fractionated from scorpion venoms had the same HPLC mobility or produced the same functional modifications of ryanodine receptors as seen with RyTx.

The conductance change induced by RyTx was similar to that produced by the alkaloid ryanodine and consisted of a long-lived substate with a conductance ~2.3-fold lower than the open state conductance. The stimulation of [^{3}H]ryanodine binding by RyTx can be explained on the basis of the increase in open and substate probabilities produced by the peptide under the assumption that open and substate conformations but not closed conformations favor the binding of ryanodine. A concentration of 1 μM RyTx decreased the probability of the open state from 0.21 to 0.13 and, at the same time, increased the probability of the substate from null to 0.38 (Fig. 3). Thus the probability of the conducting states induced by RyTx, assumed to represent a favorable conformation for the binding of ryanodine, increased from 0.21 to 0.51, or 2.4-fold. The latter increase in probability was similar to the ~3-fold stimulation of [^{3}H]ryanodine binding produced by 1 μM RyTx (Fig. 10).

Ligand binding analysis indicated that the pharmacological effects of RyTx and ryanodine did not originate from binding of these ligands to the same site(s) on the receptor. This was demonstrated by the fact that RyTx did not change

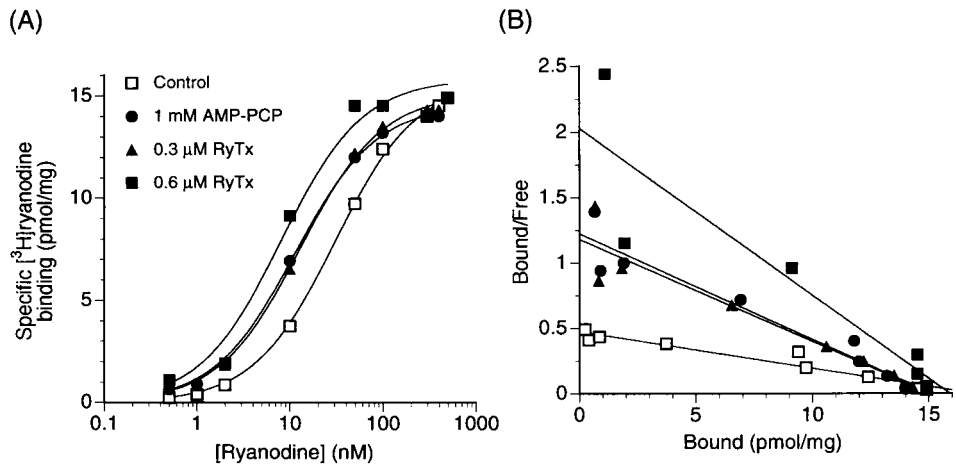

FIGURE 12 Analysis of ryanotoxin stimulation of [^{3}H]ryanodine binding. (*A*) Equilibrium binding was performed in the absence (□) or presence of 1 mM AMP-PCP (●), 0.3 μM RyTx (▲), or 0.6 μM RyTx (■). Solid lines represent a fit using a single binding site isotherm to averages of three experiments. Fitted parameters were B_{max} = 17 ± 2.2 pmol/mg and K_d = 37.7 ± 4.9 nM (control); 15.1 ± 1.4 pmol/mg and 12.5 ± 1.2 nM (AMP-PCP); 15.1 ± 1.5 pmol/mg and 12.9 ± 1.3 nM (0.3 μM RyTx); 16.2 ± 4.8 pmol/mg and 9.8 ± 3 nM (0.6 μM RyTx). (*B*) Representation of the same data and fit in Scatchard format.

the B_{max} of high-affinity [^{3}H]ryanodine binding at equilibrium. It is also unlikely that RyTx competed for binding to the low-affinity ryanodine-binding site(s) described elsewhere (Lai et al., 1989; Pessah and Zimanyi, 1991; Wang et al., 1993), because micromolar concentrations of unlabeled RyTx stimulated rather than inhibited high-affinity [^{3}H]ryanodine binding. Thus micromolar concentrations of RyTx kept the ryanodine receptor open, whereas ryanodine binding to the low-affinity ryanodine-binding site(s) closes the channel (see references above). However, because the highest toxin concentration tested (10 μM) may not be sufficient to occupy all of the low-affinity ryanodine-binding sites, we cannot exclude the possibility that RyTx may bind to low-affinity ryanodine-binding sites with dissociation constants of >10 μM. Higher concentrations of RyTx may be required to determine whether the peptide modifies the channel in a manner similar to that produced by ryanodine binding to low-affinity sites.

There are several kinetic features established by radioligand binding analysis, single-channel recording, and Ca^{2+} fluxes that quantitatively distinguished the actions of RyTx from those of ryanodine. The fact that channels in the presence of RyTx alternated between open, closed, and peptide-modified states strongly suggested that RyTx could freely associate and dissociate from the channel. This is in contrast to the known effect of ryanodine, which, by binding irreversibly, locks the channel permanently in the substate. The reversible binding of RyTx was directly demonstrated by SR washout experiments and could readily explain the delayed inhibition of RyTx-modified channels by ruthenium red. Studies using ryanodine have demonstrated that the alkaloid induces a substate insensitive to ruthenium red (Imagawa et al., 1987; Nagasaki and Fleischer, 1988; Ma, 1993). Assuming the RyTx-induced substate is also insensitive to the blocker, the channel must leave the substate and enter the open state to become blocked by ruthenium red. Because the probability of the substate was higher than that of the open state, the block by ruthenium red may have been delayed until a sufficiently long burst of openings occurred. Inspection of the diary of openings (Fig. 7 *C*) indicated that, in fact, two bursts of openings took place immediately before the block of the RyTx-modified channel by ruthenium red. In addition, the pharmacological onset was much faster for RyTx than for ryanodine. In single-channel recordings, the time of onset of the substate was almost instantaneous for RyTx, but required no less than 2 min, and up to 15 min in the case of ryanodine. In fura-2 experiments in vesicles, RyTx caused an immediate release of SR Ca^{2+}, whereas 100 nM ryanodine had no effect after 5 min of incubation (not shown). These findings suggest that the association kinetics of RyTx with the channel may be much faster than the association kinetics of ryanodine. A simple explanation for the faster kinetics of RyTx binding would be that more conformations of the ryanodine receptor (open, closed, or spontaneous substates) permit peptide binding than ryanodine binding.

Ca^{2+} transients in myotubes dialyzed with 5 μM RyTx were potentiated such that the peak free Ca^{2+} was larger than that of controls and the removal phase was slower than that of controls. The slowing of removal was apparent from a comparison of scaled traces (not shown) and from the fact that Ca^{2+} remained near the maximum level for several hundreds of milliseconds after stimulation. In contrast, removal was immediately obvious in control cells after stimulation. The slowing of removal was consistent with the observation in planar bilayers that RyTx prolonged the opening of the ryanodine receptor channel and, in so doing, tipped the net Ca^{2+} transport balance in the direction of release. Interestingly, the resting fluorescence of cells dyalized with RyTx was not modified. This result suggests that the average concentration of RyTx in cells may have not reached the micromolar range, and therefore closed channels were not opened by the toxin, as shown in planar bilayer and SR Ca^{2+} flux experiments. On the other hand, it is entirely possible that RyTx dialyzed into cells was able to bind channels and thus prolong Ca^{2+} release, once these channels were open, by the voltage sensor or by cytoplasmic Ca^{2+} released from the SR. Because in the skeletal muscle cell, the activation and well as the inactivation of Ca^{2+} release are under the control of the voltage sensor (Rios et

al., 1991), RyTx bound to ryanodine receptors may have altered either or both processes.

A potentiation of the Ca^{2+} transient could have also resulted from a possible stimulation of Ca^{2+} entry into the cell by the toxin. However, this was unlikely because as indicated above, the resting fluorescence of cells dialyzed with RyTx was not affected. In addition, in whole-cell recordings of myotubes under voltage clamp, RyTx did not produced a noticeable effect on L-type or T-type Ca^{2+} currents (not shown). Furthermore, the voltage dependence of the Ca^{2+} transient in control and dialyzed cells was indicative of a purely voltage-dependent and not a Ca^{2+} entry mechanism. Studies of dysgenic skeletal myotubes expressing cardiac L-type Ca^{2+} channels have shown that Ca^{2+} transients in these cells are a graded function of the L-type Ca^{2+} current (Garcia et al., 1994). This is demonstrated by the fact that step potentials above +20 mV curtailed the Ca^{2+} transient as the driving force for Ca^{2+} entry into the cell was reduced (Garcia et al., 1994). In the present study, Ca^{2+} transients did not diminish at positive potentials either in control or toxin dialyzed cells, and therefore a Ca^{2+} entry mechanism could not possibly explain the potentiation of the Ca^{2+} transient.

Small venom-derived peptides such as imperatoxin A (H. Valdivia et al., 1992) or peptide A derived from the amino-terminal portion of the II-III loop of the α_1 subunit of the DHP receptor (Lu et al., 1994; El-Hayek et al., 1995) have been shown to stimulate opening of the ryanodine receptor channel at relatively low concentrations. Both types of peptides demonstrate a tissue specificity that leads to the activation of skeletal but not cardiac ryanodine receptors. This may be indicative of a common binding domain on the skeletal isoform. Because the increase in activity produced by imperatoxin A or the II-III loop peptide was not associated with changes in single-channel conductance, the pharmacological action of RyTx may be indicative of a separate binding domain for the latter peptide. Ligand binding competition between different venom-derived peptides and the II-III loop peptide may be used to establish the functional relations between these putative binding sites. Although the functional significance of these peptide-binding domains is currently unknown, these studies may ultimately serve to identify domains of the ryanodine receptor stimulated during skeletal-type excitation-contraction coupling.

Supported by National Institutes of Health grants GM36852 and HL 47053. MB is a recipient of a postdoctoral fellowship from the Philippe Foundation.

REFERENCES

Adams, M. E., and G. Swanson. 1994. Neurotoxins. *Trends Neurosci.* 17(Suppl.):1–28.

Bean, B. P. 1984. Nitrendipine block of cardiac calcium channels: high affinity binding to the inactivated state. *Proc. Natl. Acad. Sci. USA.* 81:6388–6392.

Callaway, C., A. Seryshev, J-P. Wang, K. J. Slavik, D. H. Needleman, C. I. Cantu, Y. Wu, T. Jayaraman, A. R. Marks, and S. L. Hamilton. 1994. Localization of the high and low affinity [^{3}H]ryanodine binding sites on the skeletal muscle Ca^{2+} release channel. *J. Biol. Chem.* 269: 15876–15884.

Carroll, S., J. Skarmeta, X. Yu, K. Collins, and G. Inesi. 1991. Interdependence of ryanodine binding, oligomeric receptor interactions, and Ca^{2+} release regulation in junctional sarcoplasmic reticulum. *Arch. Biochem Biophys.* 290:239–247.

Chen, S. R. W., L. Zhang, and D. H. Maclennan. 1993. Antibodies as probes for Ca^{2+} activation site in the Ca^{2+} release channel (ryanodine receptor) of rabbit skeletal muscle sarcoplasmic reticulum. *J. Biol. Chem.* 268:13414–13421.

Cognard, C., M. Rivet-Bastide, B. Constantin, and G. Raymond. 1992. Progressive dominance of "skeletal" versus "cardiac" types of excitation-contraction coupling during in vitro skeletal myogenesis. *Pflugers Arch.* 422:207–209.

Coronado, R., S. Kawano, C. J. Lee, C. Valdivia, and H. H. Valdivia. 1992. Planar bilayer recording of ryanodine receptors of sarcoplasmic reticulum. *Methods Enzymol.* 207:699–707.

Coronado, R., J. Morrissette, M. Sukhareva, and D. M. V. Vaughan. 1994. Invited review: structure and function of ryanodine receptors. *Am. J. Physiol.* 266:C1485–C1505.

Ebashi, S. 1991. Excitation-contraction coupling and the mechanism of muscle contraction. *Annu. Rev. Physiol.* 53:1–16.

El-Hayek, R., B. Antoniu, J. Wang, S. L. Hamilton, and N. Ikemoto. 1995. Identification of calcium release-triggering and blocking regions of the II-III loop of the skeletal muscle dihydropyridine receptor. *J. Biol. Chem.* 270:22116–22118.

Fabiato, A. 1988. Computer programs for calculating total from specified free or free from specified total ionic concentrations in aqueous solutions containing multiple metals and ligands. *Methods Enzymol.* 157:387.

Fleischer, S., and M. Inui. 1989. Biochemistry and biophysics of excitation-contraction coupling. *Annu. Rev. Biophys. Biophys. Chem.* 18: 333–364.

Garcia, J., and K. G. Beam. 1994. Measurement of calcium transients and slow calcium current in myotubes. *J. Gen. Physiol.* 103:107–123.

Garcia, J., T. Tanabe, and K. G. Beam. 1994. Relationship of calcium transients to calcium currents and charge movements in myotubes expressiong skeletal and cardiac dihydropyridine receptors. *J. Gen. Physiol.* 103:125–147.

Grouselle, M., J. Koenig, M. L. Lascombe, J. Chapron, D. Meleard, and D. Georgescauld. 1991. Fura-2 imaging of spontaneous and electrically induced oscillations of intracellular free Ca^{2+} in rat myotubes. *Pflugers Arch.* 418:40–50.

Grynkiewicz, G., M. Poenie, and R. Y. Tsien. 1985. A new generation of Ca^{2+} indicators with greatly improved fluorescence properties. *J. Biol. Chem.* 260:3440–3450.

Hamilton, S. L., A. Yatani, K. Brush, A. Schwartz, and A. M. Brown. 1987. A comparison between the binding and electrophysiological effects of dihydropyridines on cardiac membranes. *Mol. Pharmacol.* 31: 221–231.

Imagawa, T., J. Smith, R. Coronado, and K. Campbell. 1987. Purified ryanodine receptor from muscle sarcoplasmic reticulum is the Ca^{2+}-permeable pore of the calcium release channel. *J. Biol. Chem.* 262: 16636–16643.

Inui, M., S. Wang, A. Saito, and S. Fleischer. 1988. Characterization of junctional and longitudinal sarcoplasmic reticulum from heart muscle. *J. Biol. Chem.* 263:10843–10850.

Jayaraman, T., A. M. Brillantes, A. P. Timerman, S. Fleischer, H. Erdjument-Bromage, P. Tempst, and A. R. Marks. 1992. FK506 binding protein associated with the calcium release channel (ryanodine receptor). *J. Biol. Chem.* 267:9474–9477.

Lacinova, L., A. L. Bosse, V. Flockerzi, and F. Hofmann. 1995. The block of the expressed L-type calcium channel is modulated by the β_3 subunit. *FEBS Lett.* 373:103–107.

Laemmli, U. K. 1970. Cleavage of structural proteins during the assembly of the head of bacteriophage T4. *Nature.* 227:680–685.

Lai, F., H. Erickson, E. Rousseau, Q-Y. Liu, and G. Meissner. 1988. Purification and reconstitution of the calcium release channel from skeletal muscle. *Nature.* 331:315–319.

Lai, F., M. Misra, L. Xu, H. Smith, and G. Meissner. 1989. The ryanodine receptor-Ca^{2+} release channel complex of skeletal muscle sarcoplasmic

reticulum. Evidence for a cooperatively coupled, negatively charged homotetramer. *J. Biol. Chem.* 264:16776–16785.

Lester, D., P. Lazarovici, M. Pelhate, and E. Zlotkin. 1982. Purification, characterization and action of two insect toxins from the venom of the scorpion *Buthotus judaicus*. *Biochim. Biophys. Acta.* 701:370–381.

Lu, X., L. Xu, and G. Meissner. 1994. Activation of the skeletal muscle calcium release channel by a cytoplasmic loop of the dihydropyridine receptor. *J. Biol. Chem.* 269:6511–6516.

Ma, J. 1993. Block by ruthenium red of the ryanodine-activated calcium release channel of skeletal muscle. *J. Gen. Physiol.* 102:1031–1056.

McPherson, P. S., and H. P. Campbell. 1990. Solubilization and biochemical characterization of the high affinity [^{3}H]ryanodine receptor from rabbit brain microsomes. *J. Biol. Chem.* 265:18454–18460.

McPherson, P. S., and K. P. Campbell. 1993. The ryanodine receptor/Ca^{2+} release channel. *J. Biol. Chem.* 268:13765–13768.

Meissner, G. 1994. Ryanodine receptors/Ca^{2+} release channels and their regulation by endogenous effectors. *Annu. Rev. Physiol.* 56:485–508.

Morrissette, J., and R. Coronado. 1994. Isolation and characterization of ryanotoxin, a peptide from the scorpion *Buthotus judaicus* which mimics the action of ryanodine on Ca^{2+} release channels. *Biophys. J.* 66:A415.

Morrissette, J., J. Kratzschmar, B. Haendler, R. El-Hayek, J. Mochca-Morales, B. M. Martin, J. R. Patel, R. L. Moss, W-D. Schleuning, R. Coronado, and L. D. Possani. 1995. Primary structure and properties of helothermine, a peptide toxin that blocks ryanodine receptors. *Biophys. J.* 68:2280–2288.

Nagasaki, K., and S. Fleischer. 1988. Ryanodine sensitivity of the calcium release channel of sarcoplasmic reticulum. *Cell Calcium.* 9:1–7.

Ogawa, Y. 1994. Role of ryanodine receptors. *Crit. Rev. Biochem. Mol. Biol.* 29:229–274.

Pessah, I., A. Francini, D. Scales, A. Waterhouse, and J. Casida. 1986. Calcium-ryanodine receptor complex. Solubilization and partial characterization from skeletal muscle junctional sarcoplasmic reticulum vesicles. *J. Biol. Chem.* 261:8643–8648.

Pessah, I., A. Waterhouse, and J. Casida. 1985. The calcium-ryanodine receptor complex of skeletal and cardiac muscle. *Biochem. Biophys. Res. Commun.* 128:449–456.

Pessah, I., and I. Zimanyi. 1991. Characterization of multiple [^{3}H]ryanodine-binding sites on the Ca^{2+} release channel of sarcoplasmic reticulum from skeletal and cardiac muscle: evidence for a sequential mechanism in ryanodine action. *Mol. Pharmacol.* 39:679–689.

Rios, E., J. Ma, and A. Gonzalez. 1991. The mechanical hypothesis of excitation contraction (EC) coupling in skeletal muscle. *J. Muscle Res.* 12:127–137.

Rios, E., and G. Pizarro. 1991. Voltage sensor of excitation-contraction coupling in skeletal muscle. *Pharmacol. Rev.* 71:849–908.

Stern, M. D., and E. G. Lakatta. 1992. Excitation-contraction coupling in the heart: the state of the question. *FASEB J.* 6:3092–3100.

Sukhareva, M., J. Morrissette, and R. Coronado. 1994. Mechanism of chloride-dependent release of Ca^{2+} in the sarcoplasmic reticulum of rabbit skeletal muscle. *Biophys. J.* 67:751–765.

Takekura, H., L. Bennett, K. Tanabe, K. G. Beam, and C. Franzini-Armstrong. 1994. Restoration of junctional tetrads in dysgenic myotubes by dihydropyridine receptor cDNA. *Biophys. J.* 67:793–803.

Tanabe, T., K. G. Beam, B. A. Adams, T. Niidome, and S. Numa. 1990. Regions of the skeletal muscle dihydropyridine receptor critical for excitation-contraction coupling. *Nature.* 346:567–572.

Valdivia, C., D. Vaughan, B. V. L. Potter, and R. Coronado. 1992. Fast release of $^{45}Ca^{2+}$ induced by inositol 1,4,5-trisphosphate and Ca^{2+} in the sarcoplasmic reticulum of rabbit skeletal muscle: evidence for two types of Ca^{2+} release channels. *Biophys. J.* 61:1184–1193.

Valdivia, H. H., O. Fuentes, R. El-Hayek, J. Morrissette, and R. Coronado. 1991. Activation of the ryanodine receptor Ca^{2+} release channel of sarcoplasmic reticulum by a novel scorpion venom. *J. Biol. Chem.* 266:19135–19138.

Valdivia, H. H., M. S. Kirby, W. J. Lederer, and R. Coronado. 1992. Scorpion toxins targeted against the sarcoplasmic reticulum Ca^{2+}-release channel of skeletal and cardiac muscle. *Proc. Natl. Acad. Sci. USA.* 89:12185–12189.

Wang, J. P., D. H. Needleman, and S. L. Hamilton. 1993. Relationship of low affinity [^{3}H]ryanodine binding sites to high affinity sites on the skeletal muscle Ca^{2+} release channel. *J. Biol. Chem.* 268:20974–20982.

Wier, W. G., T. M. Egan, J. R. Lopez-Lopes, and C. W. Blake. 1994. Local control of excitation-contraction coupling. *J. Physiol. (Lond.).* 474: 463–471.

Witcher, D. R., P. S. McPherson, S. D. Kahl, T. Lewis, P. Bentley, M. J. Mullinnix, J. D. Windass, and K. P. Campbell. 1994. Photoaffinity labeling of the ryanodine receptor/Ca^{2+} release channel with an azido derivative of ryanodine. *J. Biol. Chem.* 269:13076–13079.

Zimanyi, I., and I. Pessah. 1991. Comparison of [^{3}H]ryanodine receptors and Ca^{2+} release from rat cardiac and rabbit skeletal muscle sarcoplasmic reticulum. *J. Pharmacol. Exp. Ther.* 256:938–946.

Zimanyi, I., and I. N. Pessah. 1992. Pharmacological characterization of the specific binding of [^{3}H]ryanodine to rat brain microsomal membranes. *Brain Res.* 561:181–191.

Zorzato, F., J. Fujii, K. Otsu, M. Phillips, N. M. Green, F. A. Lai, G. Meissner, and D. H. MacLennan. 1990. Molecular cloning of cDNA encoding human and rabbit forms of the Ca^{2+} release channel (ryanodine receptor) of skeletal muscle sarcoplasmic reticulum. *J. Biol. Chem.* 265:2244–2256.